NOTES AND CORRESPONDENCE

The Interactions between a Midlatitude Blocking Anticyclone and Synoptic-Scale Cyclones That Occurred during the Summer Season

ANTHONY R. LUPO AND PHILLIP J. SMITH

Department of Earth and Atmospheric Sciences, Purdue University, West Lafayette, Indiana

20 September 1996 and 2 May 1997

ABSTRACT

Using the Goddard Laboratory for Atmospheres Goddard Earth Observing System 5-yr analyses and the Zwack–Okossi equation as the diagnostic tool, the horizontal distribution of the dynamic and thermodynamic forcing processes contributing to the maintenance of a Northern Hemisphere midlatitude blocking anticyclone that occurred during the summer season were examined. During the development of this blocking anticyclone, vorticity advection, supported by temperature advection, forced 500-hPa height rises at the block center. Vorticity advection and vorticity tilting were also consistent contributors to height rises during the entire life cycle. Boundary layer friction, vertical advection of vorticity, and ageostrophic vorticity tendencies (during decay) consistently opposed block development. Additionally, an analysis of this blocking event also showed that upstream precursor surface cyclones were not only important in block development but in block maintenance as well.

In partitioning the basic data fields into their planetary-scale (P) and synoptic-scale (S) components, 500-hPa height tendencies forced by processes on each scale, as well as by interactions (I) between each scale, were also calculated. Over the lifetime of this blocking event, the S and P processes were most prominent in the blocked region. During the formation of this block, the I component was the largest and most consistent contributor to height rises at the center point. It was also shown that the height-rise regions located on the anticyclonic side of the jet maxima associated with block development and intensification were primarily composed of the S and I components. Also, the precursor cyclones were associated with S or S and I height rises that contributed to the formation of this block. Finally, the results of this paper show that the forcing associated with summer-season blocking events are similar to that of their winter-season counterparts neglecting the natural case-to-case variability. In comparing these results to the results of other papers in this series, however, it is suggested that there may be two models for block development.

1. Introduction

Blocking anticyclones are large-scale phenomena that can have a significant impact on midlatitude weather conditions and regional climates not only over the areas they cover, but upstream and downstream as well (e.g., Rex 1950a,b; Illari 1984; Quiroz 1984; Agayan and Mokhov 1989). In recent years, the dynamic link between blocking anticyclones and upstream synoptic-scale surface cyclones has been a subject of intense interest in both model and observational studies (e.g., Frederiksen 1982; Shutts 1983, 1986; Colucci 1985, 1987; Egger et al. 1986; Mullen 1987; Tracton 1990; Alberta et al. 1991). Despite this interest, relatively few [e.g., Konrad and Colucci 1988; Tsou and Smith 1990; Lupo and Smith 1995b (hereafter LS95b); Lupo 1997 (hereafter L97)] have investigated the dynamic connection between the development of a particular surface cyclone event and block formation and/or maintenance.

Diagnostic studies (e.g., Alberta et al. (1991); Tsou and Smith (1990); Tracton (1990); and LS95b) have shown that anticyclonic vorticity advection was important in block formation. The former two, and L97, have also noted the importance of temperature advection in block formation, but all three studies found that once the block was established, barotropic processes dominated the maintenance of the event. Tsou and Smith (1990), Alberta et al. (1991), and LS95b also found block formation to be preceded by a rapid or explosively developing surface cyclone. Additionally, Tsou and Smith (1990) noted the importance of a developing jet streak just prior to block onset in enhancing the anticyclonic vorticity advection field during block development. This block formation scenario has been supported by the findings of Lupo and Smith (1995a,b) and L97.

Since blocking has been shown to involve both synoptic-scale and planetary-scale processes, some observational studies have attempted to isolate the contributions of each and to examine the interactions between

Corresponding author address: Dr. Anthony R. Lupo, Department of Soil and Atmospheric Science, 204 Gentry Hall, University of Missouri—Columbia, Columbia, MO 65211.
E-mail: snrlupo@showme.missouri.edu

the two scales. Tsou and Smith (1990) used a partitioned form of the height tendency equation to examine the role that each scale and their interactions played in block formation. They found that the interaction component, dominated by the advection of synoptic-scale anticyclonic vorticity by the planetary-scale winds, was the largest contributor to block formation, a result supported by LS95b. Tsou and Smith (1990) also showed that block formation was the result of the superposition of a mobile and amplifying synoptic-scale ridge and a large-scale, stationary planetary-scale ridge. Tracton (1990) used a spectral decomposition of 500-hPa height fields to demonstrate that blocking reflects the superposition of synoptic-scale (and smaller scale) and planetary-scale wave modes. He used the quasigeostrophic vorticity and omega equations as the basic framework of his investigation in finding results similar to the scale partitioned results of Tsou and Smith (1990).

Many of the observational studies mentioned above focused on the development of blocking anticyclones, while only a few have examined their maintenance (e.g., Alberta et al. 1991) or decay (Dole 1986; LS95b; L97). Considering the difficulty that models encounter in successfully forecasting block formation and decay (e.g., Tibaldi and Molteni 1990; Tracton 1990; Tibaldi et al. 1993, 1994), there is *clearly* a need for more studies involving the *entire* life cycle of blocking anticyclones (Tracton 1990). Therefore, the study described here has two principal objectives: The first is to apply a diagnostic methodology involving the use of the Zwack–Okossi vorticity tendency equation (Zwack and Okossi 1986; Lupo et al. 1992) to a warm-season Northern Hemisphere midlatitude blocking anticyclone over its entire life cycle and compare these results to other published studies of blocking events, especially those of Iliari (1984) who also examined summer-season blocking over Europe. Most of the diagnostic studies referenced above focus on cold-season blocking events; however, as shown by climatological studies (e.g., Lupo and Smith 1995a), a small but significant number of blocking events do occur in the warm season. The second is to demonstrate the applicability of the Tsou and Smith (1990) block formation paradigm to a summer-season blocking event.

2. Analyses

The analyses used in this investigation were obtained from NASA/Goddard Laboratory for Atmospheres (GLA) (Schubert et al. 1993). These fields include the u and v horizontal wind vector components (m s^{-1}), geopotential height z (m), absolute temperature T, relative humidity RH, and mixing ratio q (g kg^{-1}), on a 2.0° latitude by 2.5° longitude grid at 14 mandatory pressure levels from 1000 to 20 hPa at 6-h intervals, which were then interpolated linearly in $\ln(p)$ to 50-hPa isobaric levels. Also included are a variety of surface parameters, a complete list of which can be found in Schubert et al. (1993). At the time this study was performed, the Goddard Laboratory for Atmospheres Goddard Earth Observing System (GEOS-1) analyses covered a 5-yr period from 1 March 1985 through 28 February 1990. Finally, the GLA analysis scheme incorporates data from a variety of sources, and the basic components of the assimilation system, model physics, and parameterizations used are described in more detail by Baker et al. (1987) and Schubert et al. (1993).

3. The diagnostic methods and computational procedures

The diagnosis of the blocking anticyclone was accomplished using the Zwack–Okossi (Z–O) equation (Zwack and Okossi 1986) which is a geostrophic vorticity tendency equation (Zwack and Okossi 1986) derived in its complete form by Lupo et al. (1992). This equation allows for the diagnosis of geostrophic vorticity tendency at a near-surface pressure level as forced by vertically integrated dynamic and thermodynamic forcing mechanisms, and the equation is given by

$$\left.\frac{\partial \zeta_g}{\partial t}\right|_{p_L} = \mathrm{PD}\int_{p_t}^{p_L}\left[\underbrace{-\mathbf{V}\cdot\nabla\zeta_a}_{\substack{\text{(a)}\\ \text{vadv}}} \underbrace{-\,\omega\frac{\partial\zeta_a}{\partial p}}_{\substack{\text{(b)}\\ \text{vvte}}} \underbrace{+\,\zeta_a\frac{\partial\omega}{\partial p}}_{\substack{\text{(c)}\\ \text{divh}}} \underbrace{-\,\mathbf{k}\cdot\left(\nabla\omega\times\frac{\partial\mathbf{V}}{\partial p}\right)}_{\substack{\text{(d)}\\ \text{tilt}}} \underbrace{+\,\mathbf{k}\cdot(\nabla\times\mathbf{F})}_{\substack{\text{(e)}\\ \text{fric}}} \underbrace{-\,\frac{\partial\zeta_{ag}}{\partial t}}_{\substack{\text{(f)}\\ \text{ageo}}}\right]dp$$
$$-\frac{(\mathrm{PD})R}{f}\int_{p_t}^{p_L}\left[\int_{p}^{p_L}\nabla^2\left(\underbrace{-\mathbf{V}\cdot\nabla T}_{\substack{\text{(g)}\\ \text{tadv}}} + \underbrace{\frac{\dot{Q}}{c_p}}_{\substack{\text{(h)}\\ \text{lath}}} + \underbrace{S\omega}_{\substack{\text{(i)}\\ \text{adia}}}\right)\frac{dp}{p}\right]dp. \quad (1)$$

In (1), ζ_g is the geostrophic relative vorticity, $\mathbf{V}$ the horizontal wind vector, $\dot{Q}$ the diabatic heating, S the static stability parameter $(-T/\theta)(\partial\theta/\partial p)$, ω the vertical motion (dp/dt), $\mathbf{F}$ the frictional force, ζ_a the absolute vorticity, ζ_{ag} the ageostrophic vorticity, and ∇ the del operator on an isobaric surface. The values of R, c_p, f,

T, and θ are the gas constant for dry air, the specific heat at a constant pressure, Coriolis parameter, absolute temperature, and the potential temperature, respectively. Also, PD is $(p_L - p_t)^{-1}$, where p_t is the pressure at some sufficiently high pressure level chosen to encompass most of the atmospheric mass (here 30 hPa), and p_L represents the near-surface level (the first 50-hPa pressure level above the earth's surface at any grid point). Forcing mechanisms (a)–(f) on the right-hand side of (1) are dynamic forcing mechanisms deriving from the vorticity equation, while terms (g), (h), and (i) are thermal forcing mechanisms deriving from the first law of thermodynamics (Lupo et al. 1992; Rausch and Smith 1996; L97).

Using the Z–O methodology for diagnoses at pressure levels aloft, it is necessary to express the diagnostic quantity as a geostrophic vorticity tendency equation for some specified level (e.g., $p_i = 500$ hPa) that also includes the near-surface geostrophic vorticity tendency as a forcing process [see (3) in Lupo et al. 1992]. This results in the Z–O equation for pressure levels aloft [(1) in LS95b; (2) in L97]:

$$\left.\frac{\partial \zeta_g}{\partial t}\right|_{p_i} = \left.\frac{\partial \zeta_g}{\partial t}\right|_{p_L} + \frac{R}{f}\int_{p_i}^{p_L} \nabla^2\left(-\mathbf{V}\cdot\boldsymbol{\nabla}T + \frac{\dot{Q}}{c_p} + S\omega\right)\frac{dp}{p}, \tag{2}$$

where (1) is substituted for the near-surface geostrophic vorticity tendency $\partial\zeta_g/\partial t|_{p_L}$. Finally, the vorticity tendencies resulting from (2) were then relaxed to produce height tendencies at 500 hPa, which were then spatially filtered as described below.

In (1) and (2), ω was calculated using a generalized form of the omega equation similar to the general balance-omega equation in Krishnamurti (1968):

$$\nabla^2\sigma\omega + f\zeta_a\frac{\partial^2\omega}{\partial p^2} = f\frac{\partial}{\partial p}\left(\mathbf{V}\cdot\boldsymbol{\nabla}\zeta_a - \mathbf{k}\cdot\boldsymbol{\nabla}\times\mathbf{F} + \frac{\partial\mathbf{V}}{\partial p}\times\boldsymbol{\nabla}\omega\right) + f\omega\frac{\partial^2\zeta}{\partial p^2} + \frac{R}{p}\nabla^2\left(\mathbf{V}\cdot\boldsymbol{\nabla}T - \frac{\dot{Q}}{c_p}\right), \tag{3}$$

where σ is the static stability parameter $\sigma = (-RT/p\theta)(\partial\theta/\partial p)$. This form of the omega equation was chosen because of its compatibility with (1) and (2), that is, each of the forcing processes that appear in (1) and (2) has a complement in (3). In (1), (2), and (3), diabatic heating and other quantities that must be parameterized, and the numerical methods used to calculate each quantity are treated in more detail by Lupo et al. (1992), LS95b, Rausch and Smith (1996), Rolfson and Smith (1996), or L97. The computations described here were carried out over the entire Northern Hemisphere, and smaller regions (domains of 40° latitude by 60° longitude centered as closely as possible to the block center) were chosen for examining the computed height tendencies in the blocking anticyclone and the immediate vicinity in the upstream and downstream directions.

In obtaining some of our results, it was necessary to partition the GEOS-1 analyses into ''planetary-scale'' (P) and ''synoptic-scale'' (S) components, and the scale partitioning was accomplished using a second-order, two-dimensional Shapiro (1970) filter. The procedure and characteristics of the filtering process are described in more detail by LS95b; thus, only a brief summary is given here. The filtered analyses (P and S) were used in a partitioned form of (1) and (2) derived by substituting for each variable X:

$$X = \overline{X} + X', \tag{4}$$

where $\overline{X}$ (X') are the filtered analyses (portion of the analyses filtered out) and represent the planetary (synoptic)-scale component. The scale partitioned form of (1) or (2) is given by

$$\left.\frac{\partial \zeta_g}{\partial t}\right|_{p_i} = \mathrm{P} + \mathrm{S} + \mathrm{I}. \tag{5}$$

The forcing mechanisms represented in (1) or (2) mathematically as product terms give rise to a scale-interaction (I) vorticity tendency in (5), and an example of this partitioning as applied to term (a) on the right-hand side of (1) or (2) is

$$\left.\frac{\partial \zeta_g}{\partial t}\right|_{p_i} = \left.\frac{\partial \zeta_g}{\partial t}\right|_{p_L} = \mathrm{PD}\int_{p_t}^{p_L}\Bigg(\underbrace{-\overline{\mathbf{V}}\cdot\boldsymbol{\nabla}\overline{\zeta}_a}_{\mathrm{P}} \underbrace{-\mathbf{V}'\cdot\boldsymbol{\nabla}\zeta_a'}_{\mathrm{S}} \underbrace{-\overline{\mathbf{V}}\cdot\boldsymbol{\nabla}\zeta_a'}_{\mathrm{I1}} \underbrace{-\mathbf{V}\cdot\boldsymbol{\nabla}\overline{\zeta}_a}_{\mathrm{I2}}\Bigg)\,dp, \tag{6}$$

where I1 (I2) is the advection of synoptic (planetary)-scale vorticity by the planetary (synoptic)-scale wind, and I1 + I2 equals the total interaction (I). Finally, the resultant height tendencies from (1) and (2) in section 5 were filtered in space using a fourth-order, two-dimensional Shapiro filter in order to remove small-scale ($<$1000 km, or roughly below $5\Delta x$) signal and noise present due to analysis and computational error without significantly degrading the synoptic-scale component.

4. Synoptic discussion

This summer-season blocking event, drawn from the Lupo and Smith (1995a) (hereafter LS95a) climatology (and therefore meeting their blocking criterion), occurred over Europe and Scandinavia from 15 to 20 July 1987 and was short lived and weak compared to the typical blocking event found by LS95a. Thus, this case was an ideal blocking event to study in a concise manner, and its climatological characteristics are in striking

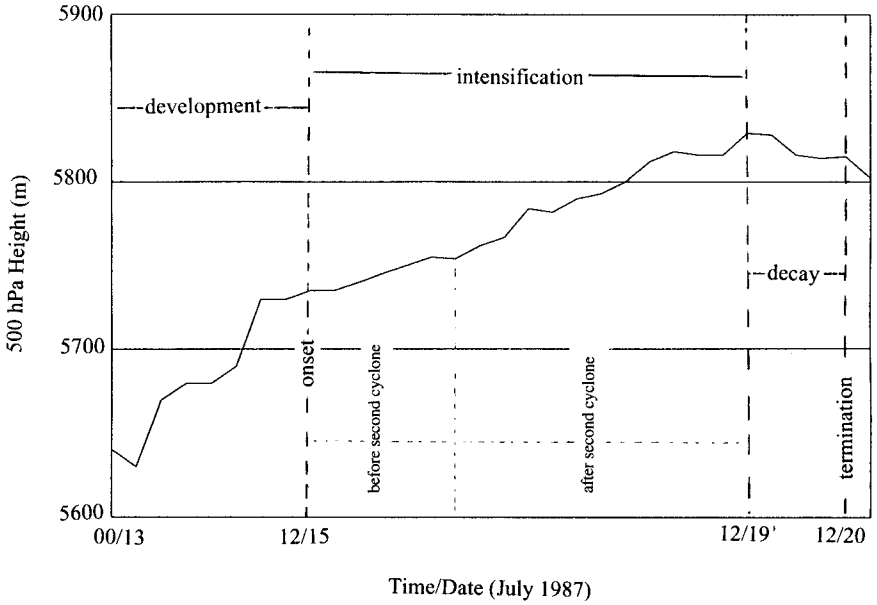

FIG. 1. Plot of the 500-hPa maximum or central height values (m) for the 500-hPa preblock ridge or blocking anticyclone vs time. Important periods of time within the block's life cycle are separated by vertical dashed lines.

contrast to the strong, longer lived blocking events examined in other studies (e.g., Illari 1984; L97). Its chronology is represented in Fig. 1, with the significant dates and periods in the blocking anticyclone's life cycle discussed in this section labeled on the *x* axis or defined inside the figure. Note that the 500-hPa central height values increased throughout the life cycle of the block until the beginning of decay, but the height rises were most rapid during the development period.

The block development period, as defined by LS95b, is the period bounded by the commencement of the 24-h period of most rapid development for the precursor cyclone and block onset. Near the start of this period, 1200 UTC 13 July 1987, an eastward propagating 500-hPa ridge was located over Iceland and the British Isles (Fig. 2a) and the movement continued so that 24 h later (not shown), the ridge was located over the North Sea. Unlike the LS95b blocking event, this ridge exhibited little visual evidence of a 500-hPa short-wave precursor ridge (see Tsou and Smith 1990). At 1200 UTC 13 July, the precursor surface cyclone (L1) was midway through the 24-h period of most rapid deepening, had deepened 6 hPa (central pressure now 992 hPa, Fig. 2a), and had moved west–northwestward to the southeast of Greenland. Cyclone L1 then became stationary after this time, and the central pressure dropped an additional 2 hPa. The 300-hPa wind field (Fig. 2a) shows that jet maxima on the western flank of a trough lay over the central Atlantic and Greenland, a favorable configuration for cyclogenesis (Rogers and Bosart 1991), but, as of this time, there is no distinguishable maximum on the upstream flank of the ridge (see Tsou and Smith 1990). In the 6 h following the end of most rapid deepening of L1 (0600 UTC 14 July), a new and robust jet maximum appeared along 15°W.

At block onset (1200 UTC 15 July), the 500-hPa large-scale ridge was located over Scandinavia (Fig. 2b). The ridge became stationary and would remain so until 18 h prior to the beginning of decay and had ended its period of most rapid development thereby intensifying at a slower rate (Fig. 1). Cyclone L1 had maintained a central pressure of 990 hPa and was now located just south of Iceland. Also, L1 was now located beneath the 500-hPa cyclone and, over the next 24 h, filled. The 300-hPa jet maximum on the upstream flank of the block (Fig. 2b) continued modest intensification up to 1200 UTC 15 July. Over the next 24 h, this jet maximum propagated up to the northwest flank of the block and, by 1200 UTC 16 July (not shown), was located over Iceland and southeast Greenland and began to weaken.

The block interacted with a second surface cyclone (L2), and 0000 UTC 18 July (Fig. 2c) was chosen to demonstrate this interaction period. Cyclone L2 was located just east of Great Britain over the North Sea (central pressure, 993). Cyclone L2 first appeared southeast of the original surface cyclone off the west coast of Ireland (central pressure, 997 hPa) on 1200 UTC 16 July, moving southeastward, then eastward across Great Britain before becoming stationary. Also, L2 deepened 5 hPa in a 6-h period (ending at 0600 UTC 17 July) to 992 hPa, but, after 0000 UTC 18 July, it began to fill. The block was centered over 70°N, 12.5°E at 0000 UTC 18 July (Fig. 2b), assuming the familiar blocking ''dipole'' pattern (e.g., the LS95b block). At this time, the 300-hPa winds (Fig. 2b) showed that the dipole was nearly girdled by a split jet (see LS95b) pattern. The

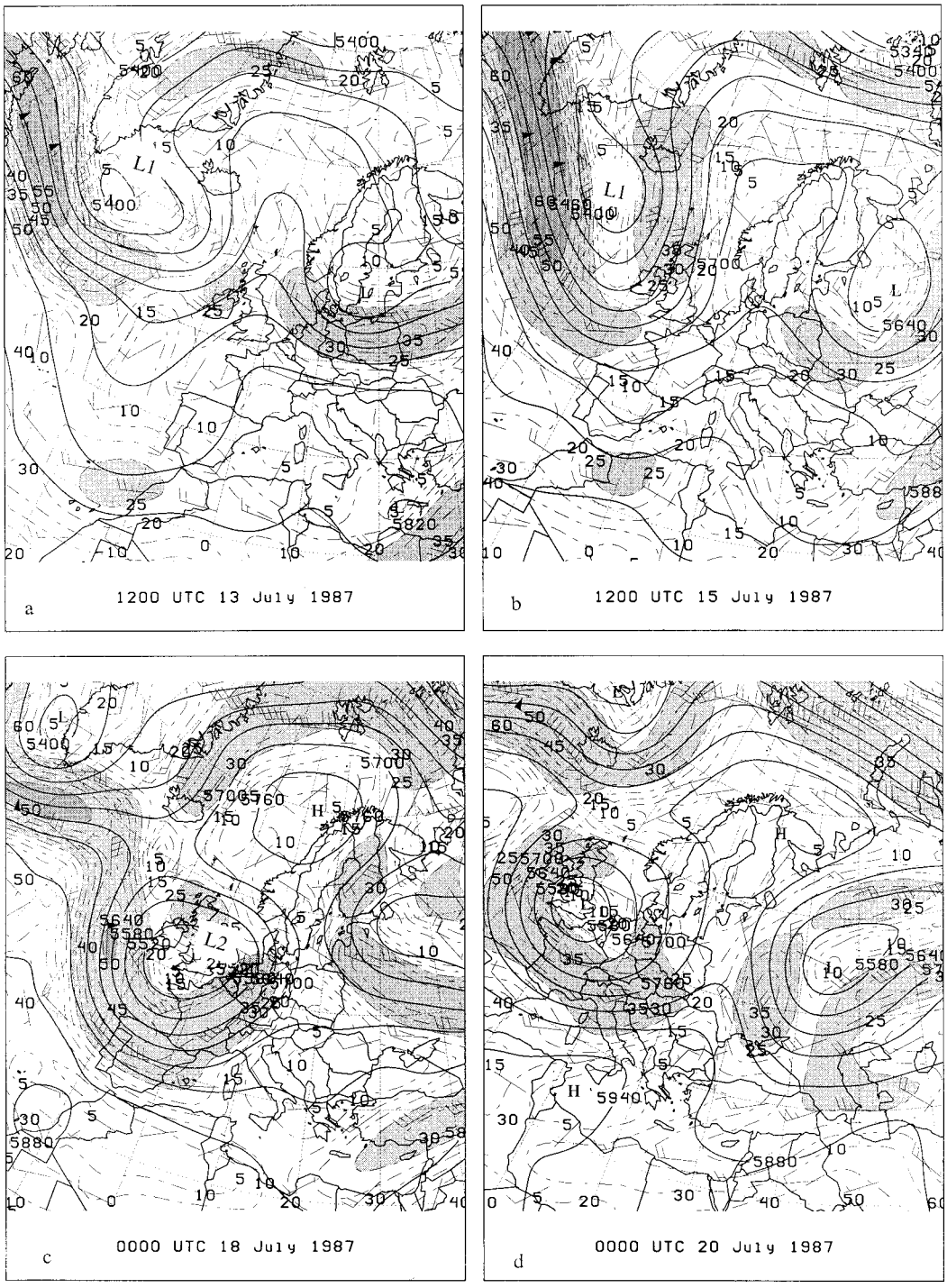

FIG. 2. Regional 500-hPa height (m) and 300-hPa wind speeds (m s^{-1}) maps for (a) 1200 UTC 13 July, (b) 1200 UTC 15 July, (c) 0000 UTC 18 July, and (d) 0000 UTC 20 July 1987. The contour intervals are 60 m for the height fields and 5 m s^{-1} for the wind speeds. The surface cyclones are denoted by L1 or L2 on the height maps. The light (dark) shaded regions 300-hPa wind speeds exceeding (25) 50 m s^{-1}. The 300-hPa wind barbs are given a full barb and flag at 10 and 50 m s^{-1}, respectively.

jet maximum located over Iceland (Fig. 2b) first appeared over Great Britain at 1200 UTC 16 July and intensified rapidly over the next 18 h. The interaction of L2 and continued intensification of the block (Fig. 1), like the development period of this and the LS95b block, resembles the development of the Tsou and Smith (1990) block.

Decay began after 1200 UTC 19 July [the time of the maximum central height value (Fig. 1)] and is represented here by 0000 UTC 20 July (Fig. 2d). The block center was located over Finland and began to drift southward (e.g., LS95b) until the block no longer met LS95a blocking criteria after 1200 UTC 20 July. Unlike the block in LS95b, the decay period was not accompanied by a rapidly developing surface cyclone upstream of the block. Like the blocks in LS95b and L97, however, there was no strong 300-hPa jet maximum located on the upstream flank of the block.

5. Diagnostic results

For brevity, the ensuing discussion focuses on composite Z–O height tendencies at the center point (highest height value) of the 500-hPa block for each of the periods identified in Fig. 1 and are displayed using bar graphs. Composite values were computed by time averaging the center-point height tendencies over each period, and the motivation for examining and partitioning the results in this manner is discussed in L97. Also, the center point was chosen for this procedure because at this point the propagation component of the height tendency is zero, and these height tendencies correspond to development. Finally, the development sum (*D*-sum) is defined as the sum of all physical processes forcing height rises, that is, positive contributors to ridge development in the bar graphs.

a. Diagnosis

The horizontal maps shown in Fig. 3 are *representative* of each period shown in Fig. 1. The development period is represented by 1200 UTC 14 July, and the ridge axis was located beneath a region of 500-hPa height rises (Fig. 3a) that encompassed all of eastern Europe and Scandinavia. This height-rise region was located on the anticyclonic shear side of the jet on the western flank of the ridge (cf. Figs. 2b and 3a). Recall that this case interacted with L2 during its life cycle (see section 4). Therefore, the midlife period of this block was divided into two subperiods (see Fig. 1) in order to examine the height tendencies before and after the development of L2. Figure 3b shows that Z–O height falls prevailed over the block center at 0000 UTC 16 July (shortly after block onset). The area of height rises associated with the development period had retreated into eastern Europe and Russia. After the development of L2 (represented by 0000 UTC 18 July), the block center was again located beneath a broad region of height rises over the northern part of the domain (Fig. 3c). This height-rise region was associated with the development of L2 and was, again, located on the anticyclonic shear side of the jet (cf. Figs. 2c and 3c) in a manner similar to that of the development period. During decay (1800 UTC 19 July), the block center was located within a region of height falls over Northern Scandinavia (Fig. 3d), and the height tendency field was generally weaker during decay than height tendency fields associated with the previous times. A region of height rises was located to the southeast of the block center (LS95b).

An examination of the composite bar graphs for the development period (Fig. 4a) shows that ageostrophic vorticity tendencies, vorticity advection, temperature advection, and vorticity tilting all contributed to height rises and block development (41%, 39%, 12%, and 8% of the development sum, respectively). The composite height tendencies for the period after block onset (before the development of L2) (Fig. 4b) show that the only two mechanisms forcing height rises were vorticity tilting (72% of the *D*-sum) and vorticity advection (28%). Temperature advection and boundary layer friction were forcing significant height falls. Note the change in sign of the temperature advection term from a contributor to block development to an inhibitor shortly following block development. After the development of L2 (Fig. 4c), vorticity advection returned to its role as a dominant height-rise mechanism at the block center (contributing 57% of the *D*-sum). Adiabatic temperature change and vorticity tilting also contributed to 500-hPa height rises during this period (24% and 19% of the *D*-sum, respectively). During decay (Fig. 4d), block center height falls were dominated by the ageostrophic tendency term. Boundary layer frictional processes also contributed to height falls at 500 hPa. Vorticity advection, temperature advection, and vorticity tilting all contributed to height rises during this period (60%, 24%, and 14% of the *D*-sum, respectively).

b. Discussion

The contributions from the various terms can be summarized for this case as follows: Vorticity advection and vorticity tilting were the most consistent contributors to height rises during this blocking event, as they were in LS95b. The results are also similar to those of Illari (1984) who found that the advection of low quasigeostrophic potential vorticity at 300 hPa was important in maintaining blocking over Europe during the summer of 1976. An examination of vertical profiles (not shown) indicated that the vorticity advection was dominated by upper-tropospheric anticyclonic vorticity advection (AVA). Further, vorticity tilting was consistently offset by the vertical advection of vorticity at the block center. While this result, the supposed ''cancellation'' of these terms, is not new, it must be stressed that these are block center-point height tendencies only. An examination of

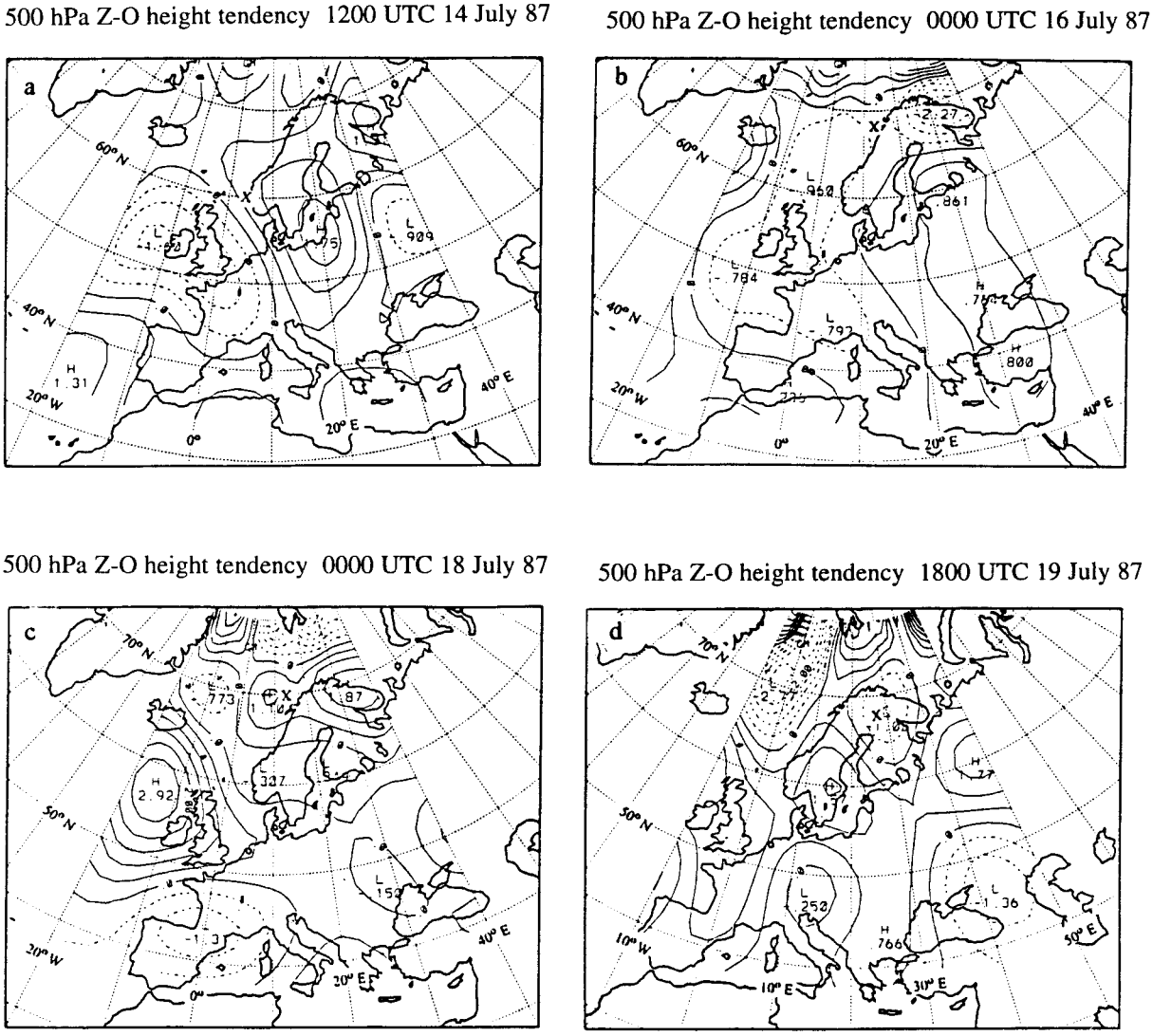

FIG. 3. Regional 500-hPa Z–O calculated total height tendency fields for (a) 1200 UTC 14 Jul, (b) 1200 UTC 16 July, (c) 0000 UTC 18 July, and (d) 1800 UTC 19 Jul 1987. The block center is marked with an "×" and the units are 0.5×10^{-3} m s^{-1}.

horizontal distributions of these terms (not shown) would not show perfect cancellation but would show some reinforcement (Grotjahn 1996). More importantly, however, the bar graphs show that these terms may not necessarily be an order of magnitude less than the more dominant terms, and, as pointed out by Grotjahn (1996), it may not be sufficient to ignore these terms based on their combined contribution. Other mechanisms consistently forcing height falls were boundary layer friction, the divergence term, and ageostrophic tendencies (especially during the decay periods for this, the LS95b, and L97 blocks). Thus, these results (for a summer-season event) are similar to those found by LS95b and other studies cited above (for winter-season events).

However, unlike the Tracton (1990) and LS95b blocking events, temperature advection played an important role in block development (Fig. 4a) (Tsou and Smith 1990; Alberta et al. 1991; L97). This mechanism was discounted by Illari (1984) as playing any significant role in the maintenance of their event, reasoning that any thermal mechanism will locally induce a pressure anomaly that changes sign with height. A representative time (1200 UTC 14 July) was chosen for further analysis of the temperature advection term revealing the scenario in which temperature advection contributed to the development of this block by forcing height rises at the ridge center (see Figs. 4a and 5a). The temperature advection profile at the ridge center (Fig. 5b, dotted) shows that lower-troposheric warm-air advection (below 300 hPa) and upper-tropospheric cold-air advection (above 300 hPa) conspired to produce 500-hPa height rises. The solid profile (Fig. 5b) is the "weighted" contribution to the 500-hPa geostrophic vorticity tendency forced by temperature advection at each level, and the total con-

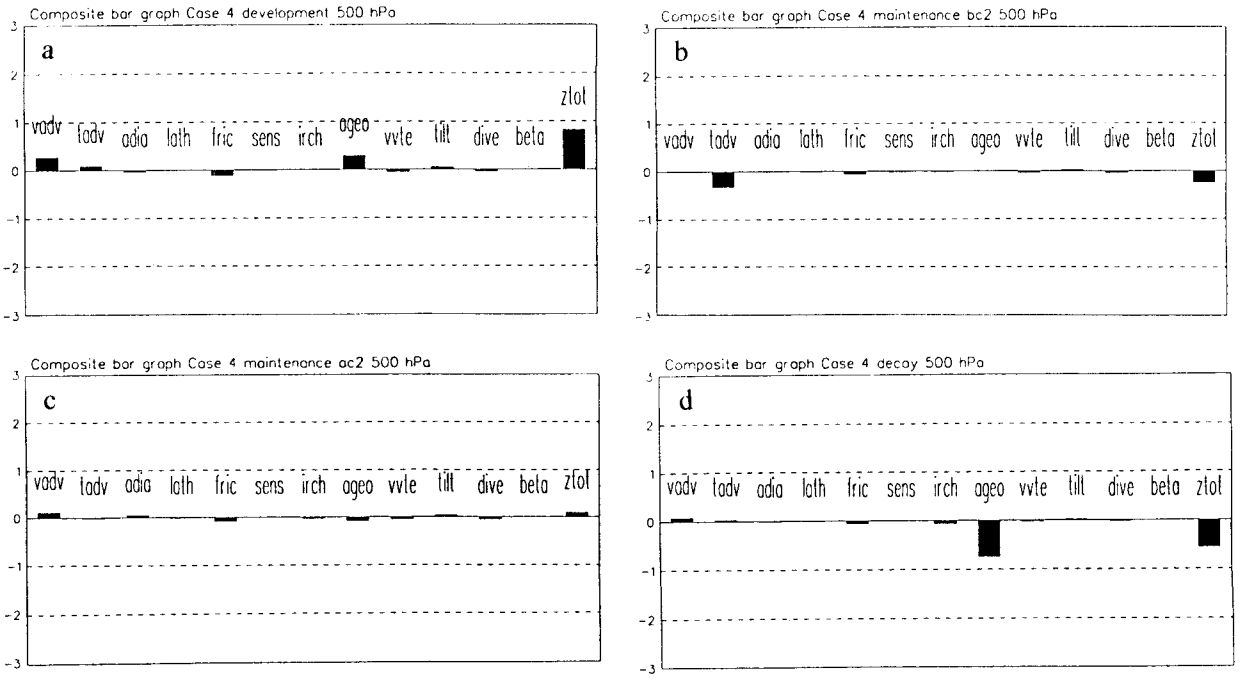

FIG. 4. Composite bar graphs for calculated 500-hPa height tendencies and each term in Eq. (1) for the (a) development, (b) intensification before cyclone development, (c) intensification after cyclone development, and (d) decay. Units are 10^{-3} m s^{-1}.

tribution to the 500-hPa vorticity tendency by temperature advection can be found simply by summing all levels (see Rausch and Smith 1996 for more details). This profile confirms that upper- and lower-tropospheric temperature advections both acted to force vorticity decreases (height increases) as the block developed. Additionally, this demonstrates the importance of vertical distribution of temperature change (as shown using the Z–O methodology) as well as horizontal distributions (through the Laplacian). As argued above, this warm-season blocking event is similar to cold-season blocking events discounting the natural case-to-case variability. As proposed by L97, however, there may be two differing models for block formation; one in which AVA (dynamic processes) dominates (Illari 1984; Tracton 1990; and LS95b) and the other in which AVA and temperature advection (dynamic and thermodynamic processes) both contribute to block formation (Tsou and Smith 1990; Alberta et al. 1991; L97).

Finally, the synoptic discussion in section 4 shows that the Tsou and Smith (1990) block formation mechanism describes the interaction between upstream surface cyclogenesis and the formation *and* intensification of this blocking event. This work also shows the association of an intervening upstream jet maximum and upper-level AVA with block development and intensification (compare to Tsou and Smith 1990; and LS95b). Therefore, the locations of jet maxima relative to the block center may be important in determining whether the block intensifies or decays since, during decay, no jet maxima were located on the upstream flank of the blocking ridge (the flow field could no longer be characterized as split flow) (see also LS95b; L97).

6. Scale partitioning results

In this section, the height tendencies are not composited as they were in section 5, since such an analysis may smooth out important features in the synoptic-scale and interaction components. Rather, regional maps and the center-point values are presented for *representative* map times for each period. First, a comparison of the 500-hPa absolute values of regional P, S, and I height tendencies (Table 1) averaged over the domains described in section 3 was performed. For this blocking event, the S (P) component was the largest (6.1×10^{-4} m s^{-1}) [second largest (3.4×10^{-4} m s^{-1})] regional contributor to the total height tendency fields, contributing 56% (31%) to the sum of the three magnitudes, while the interaction component (1.5×10^{-4} m s^{-1}) contributed only 13%. This result is not in agreement with the results of Tsou and Smith (1990), Tracton (1990), or the LS95b blocking event (Table 1). The results of Tsou and Smith (1990) and Tracton (1990) examined only the development periods, while LS95b and this study covered the entire lifetime of the blocking event. One possible explanation for the difference in the relative contribution of P, S, and I cited above could be that this blocking event occurred in the warm (summer) rather than the cold (winter) season.

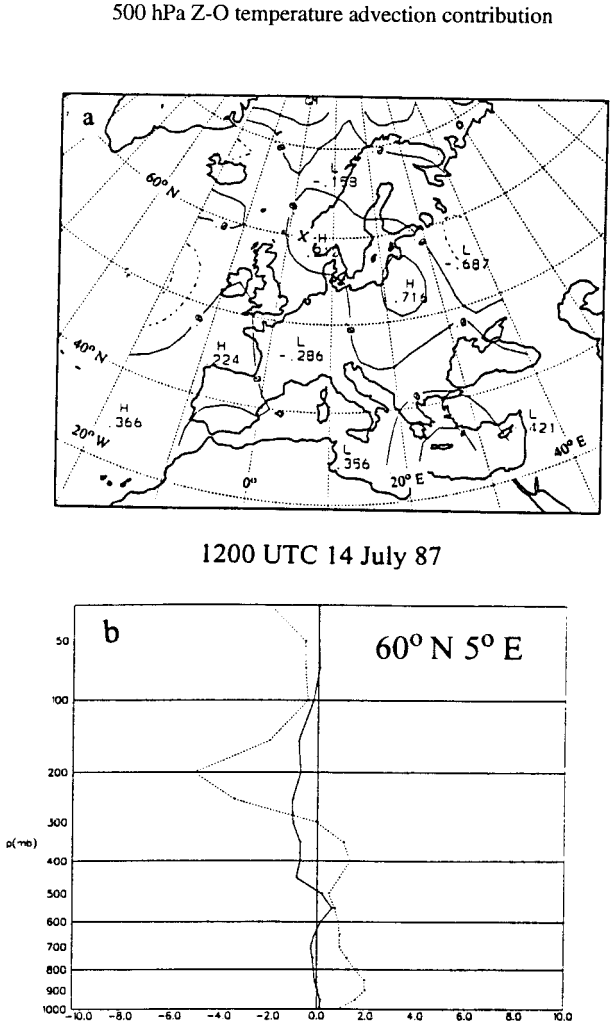

FIG. 5. (a) The contribution to the 500-hPa height tendency by temperature advection. The block center is marked with an ''×'' and the units are 0.5×10^{-3} m s^{-1}. (b) The vertical profiles of the ''weighted'' Laplacian of the temperature advection contribution at each level to the total 500-hPa geostrophic vorticity tendency ($\times 10^{-10}$ K s^{-1} m^{-2}—solid) and the temperature advection ($\times 10^{-5}$ K s^{-1}—dotted).

a. Diagnosis

The development period (1200 UTC 14 July) of this blocking event was similar to that of the LS95b block, in which the associated upstream precursor cyclone contributed to height rises through the I component. A region of height rises in the 500-hPa I height tendency field over central Europe encompassed much of the ridge axis (Fig. 6c). An examination of the P component (Fig. 6a) shows that the horizontal distribution of the height tendencies was similar to that of the total field (Fig. 3a). The S height tendency at the block center was negligible at this time (Fig. 6b) since the center was located between a height-rise region over the North Sea and Scandinavia and a height-fall region over western Europe and the eastern Atlantic. The total center-point height rises (Table 2) were forced jointly by the P and I components. A comparison of these results to the height tendencies after block development (before L2) shows (0000 UTC 16 July) the region of P height rises were weaker than in the previous period, with a larger region of P height falls located south and west of the block center (Fig. 6d). The S height tendencies (Fig. 6e) over Europe and Scandinavia similarly distributed, but of opposite sign, to those of the previous period. The I component (Fig. 6f) distribution was similar to that of the development period over the domain of interest. After block development, the associated 300-hPa jet maxima were located favorably with respect to the block center, and the S and I height-rise regions were weak and located away from the block center (see the maintenance period of the LS95b block). Table 2 shows that at this time, S and I height falls overcame P height rises at the block center.

After development of L2 (0000 UTC 18 July), 500-hPa S height rises, supported by P (Table 2), were important in forcing height rises, while the I component forced height falls at the block center. The P height tendency field (Fig. 7a) distribution was similar to the total field. The height rises at the block center were forced by S height rises (Fig. 7b), which occurred in a C-shaped region over northern Europe, Scandinavia, and Iceland. The I height rises (Fig. 7c) were occurring over the eastern Atlantic and the western flank of the

TABLE 1. Mean absolute values of the regional partitioned 500-hPa height tendencies ($\times 10^{-4}$ m s^{-1}) averaged over the life cycle of the blocking anticyclone. The entire life cycle, from development (0000 UTC 13 July) to termination (1200 UTC 20 July 1987) was considered here. This is compared to the same results for the LS95b event over the entire life cycle (1200 UTC 29 October–0000 UTC 5 November 1985).

Scale	Mean absolute value	Percent of the total
(a) This event		
Planetary (P)	3.40	31%
Synoptic (S)	6.10	56%
Interaction (I)	1.50	13%
(b) The LS95b event		
Planetary (P)	2.30	18.3%
Synoptic (S)	5.06	40.3%
Interaction (I)	5.20	41.4%

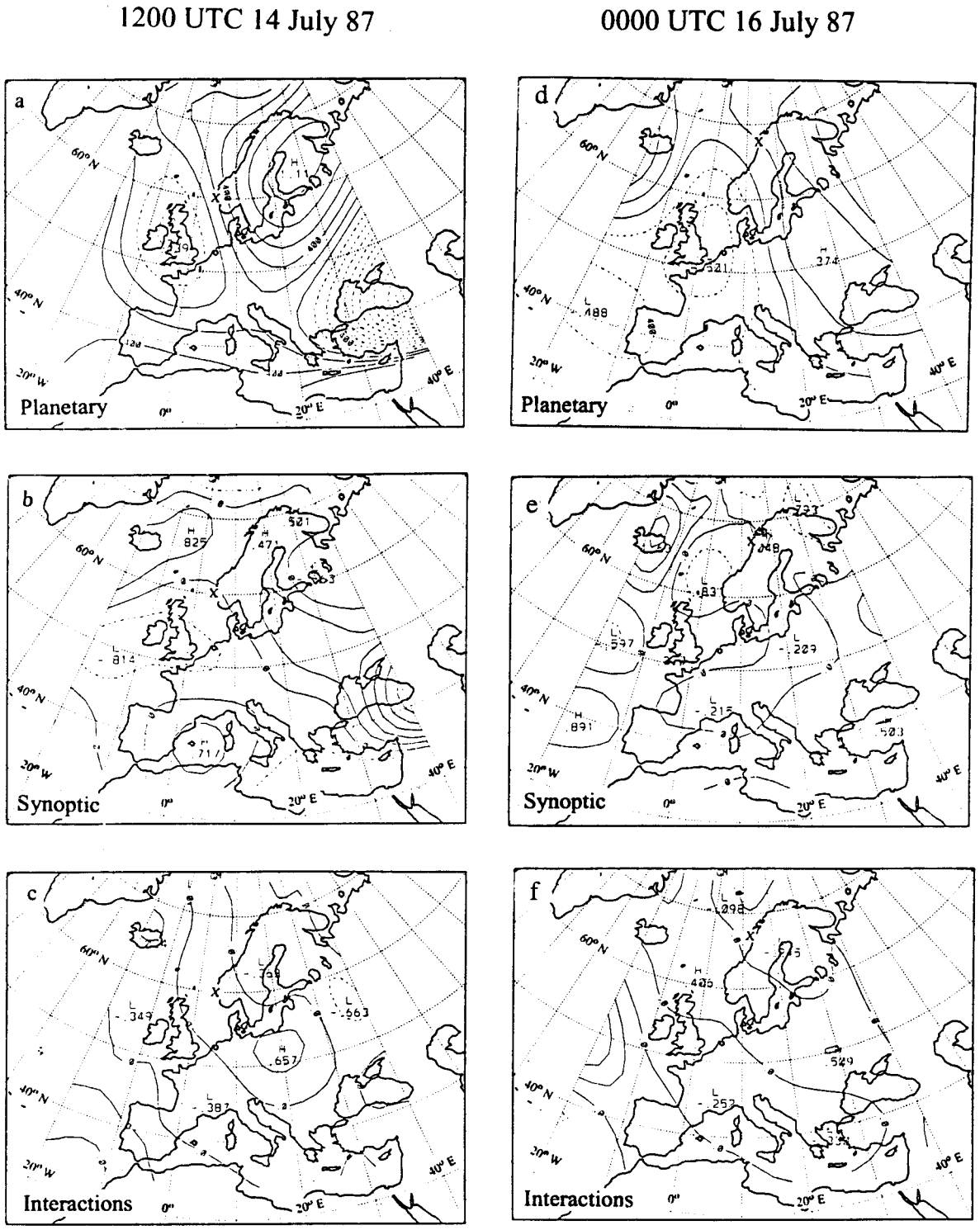

FIG. 6. The 500-hPa height tendencies as calculated by the partitioned Z–O equation for the (a) planetary-scale (P), (b) synoptic-scale (S), and (c) planetary–synoptic-scale interactions (I) are bar graphs showing the center point calculated P, S, I, and total height tendencies for 1200 UTC 14 July 1987. The block center is marked with an "×" and the units are (a) 0.2×10^{-3}, (b) and (c) 0.5×10^{-3}. Panels (d), (e), and (f) correspond to (a), (b), and (c) except for 1200 UTC July 1987.

TABLE 2. Center-point 500-hPa height tendency values for the planetary-scale (P), the synoptic-scale (S), and interaction (I) components ($\times 10^{-4}$ m s^{-1}) for each representative time.

Date	P	S	I
1200 UTC 14 July	2.44	−0.26	2.82
0000 UTC 16 July	2.18	−1.03	−1.28
0000 UTC 18 July	2.31	10.26	−1.15
1800 UTC 19 July	3.59	−11.41	−0.38

block. These results suggest that L2 was contributing to the block intensification directly through S and not through the I (P and I) component as was the case for the LS95b (this) block development. Comparing these results to height tendencies during decay (1800 UTC 19 July) showed that the S component was the prominent contributor to the height falls (Table 2) overcoming P height rises, a result unlike that of LS95b in which the P component was dominant in forcing height falls. The P height tendency field (Fig. 7d) was forcing height rises over the western three-fourths of this domain, including the region over the block center. The S height tendency field (Fig. 7e) was distributed in a similar manner to that of the total field, while the I component height tendencies were distributed in a similar manner to those of the other times examined (Fig. 7f). Finally, there were S and I height-rise regions located to the south and east of the block center (Figs. 7e,f) (similar to the LS95b block).

b. Discussion

As was found in LS95b, the height-rise regions associated with the jet maxima in block development or intensification were frequently dominated by S and/or I height rises (see Figs. 2, 3, 6, and 7). It was also shown in this section that the height rises at the block center during development and intensification were forced mainly by the I and P (development) or the S and P (intensification) components, while for the LS95b blocking event, development and intensification centerpoint height rises were forced primarily by I height rises. This suggests that in some blocking cases, the precursor cyclones may impact on block development and intensification primarily through the interaction of the synoptic scale with the planetary-scale field, while for other blocking events, the cyclones may impact more directly on block development and intensification without strong interactions between the synoptic- and the planetary-scales, that is, primarily through S or through S and I jointly. However, more study is needed to determine whether these differences are seasonal or associated with some other characteristic of blocking events. During decay, when jet maxima were no longer located on the upstream flank of the block, height-rise maxima were also located away from the block center, and, for this blocking event, (unlike LS95b) the S and I components forced height falls.

This study, like Illari (1984), demonstrates that synoptic-scale transients are important in the maintenance of observed summer-season blocking anticyclones, just as they are in their winter counterparts (e.g., Tsou and Smith 1990; LS95b). Our study used a spatially partitioned form of the Z–O equation to diagnose 500-hPa height tendencies, while Illari (1984) used a temporally partitioned form of the quasigeostrophic potential vorticity (QGPV) equation at 300 hPa. Illari (1984) found that the advection of low-potential-vorticity air northward into the blocked region (an area of low potential vorticity) was important in maintaining the block. In particular, she found that the eddy forcing on the upstream flank was important in maintaining the low (mean) PV anomaly against the tendency for it to be blown downstream. Thus, our results confirm (e.g., Illari 1984; Tsou and Smith 1990; and LS95b) that the cyclones contribute directly and/or indirectly to height rises at the block center through the S and/or the I component, respectively.

7. Conclusions

The entire life cycle of a warm-season Northern Hemisphere blocking anticyclone was examined using the Z–O equation as the diagnostic tool and the Tsou and Smith (1990) block formation model as a guide. A height tendency diagnosis using a partitioned form of the Z–O equation was also performed by separating the analyses into planetary-scale and synoptic-scale components. The principal objectives of this study were to compare the atmospheric forcing processes responsible for the formation, maintenance, and decay of this warm-season blocking event to those of cold-season cases and those of Illari (1984) and to show the applicability of the Tsou and Smith (1990) block formation model to a summer-season blocking event.

The diagnostic results of this work were compared to those of LS95b, Tsou and Smith (1990), L97, and others. This study, like many others, demonstrates the importance of midlatitude transients (e.g., extratropical cyclones) in block formation and maintenance or intensification. It was also found that anticyclonic vorticity advection, maximizing in the upper troposphere, and vorticity tilting were the largest and most consistent contributors to 500-hPa height rises at the block center throughout the block life cycle, as in LS95b and L97. Boundary layer friction and the vertical advection of vorticity were the most consistent contributors to 500-hPa height falls over the block center throughout its lifetime, while ageostrophic vorticity tendencies were the dominant mechanism forcing height falls during the decay period. Thus, this study suggests that warm- and cold-season blocking events are formed and maintained in a similar manner, discounting the natural case-to-case variability associated with any phenomenon. However, temperature advection was important in the formation of this block in agreement with the results of Tsou and

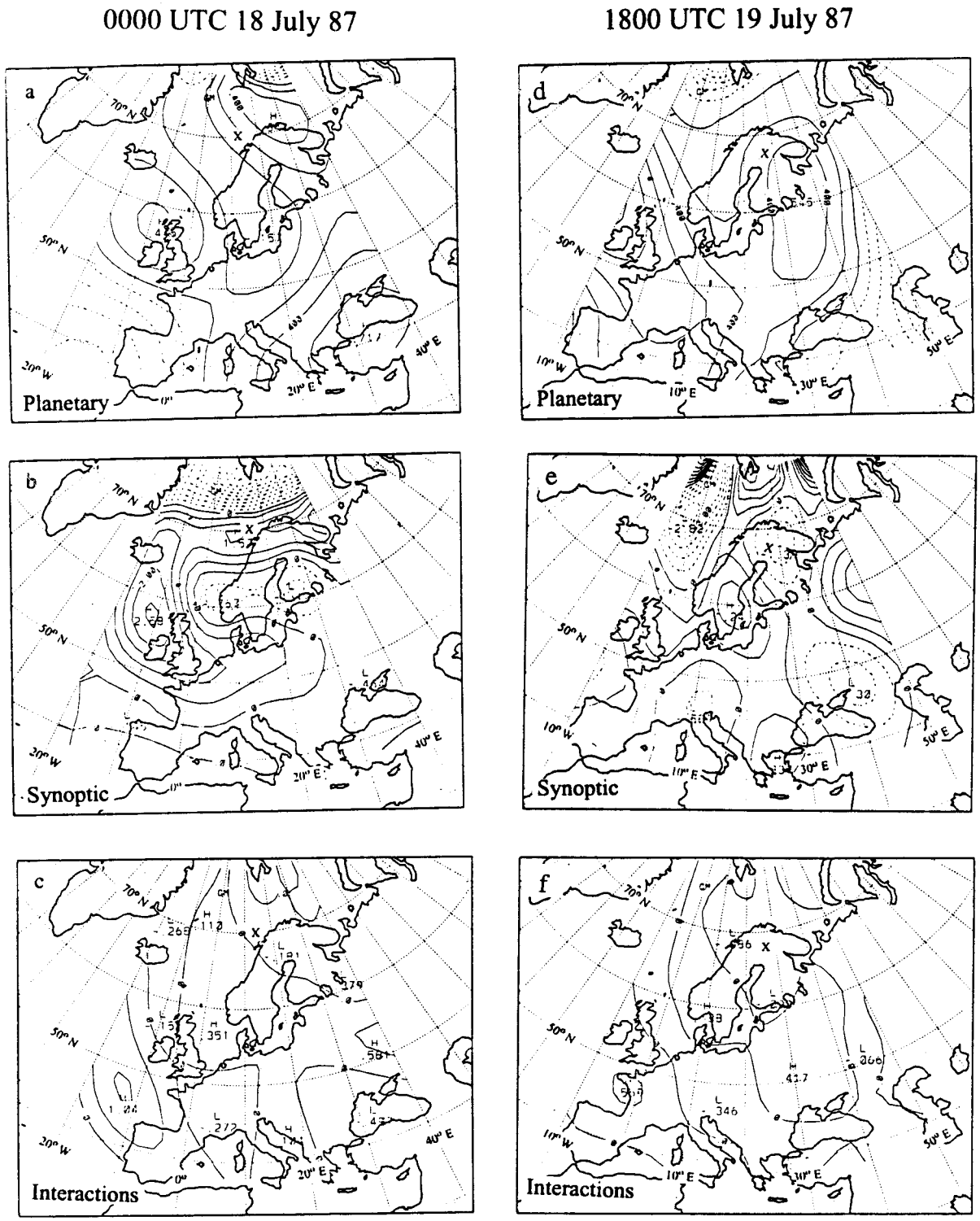

FIG. 7. As in Fig. 6 except for 0000 UTC 18 July 1987, and 1800 UTC 19 July 1987.

Smith (1990), Alberta et al. (1991), and L97. An example of the vertical distribution of temperature advection, that is, how upper-tropospheric cold-air advection and lower-tropospheric warm-air advection conspired to produce the height rises at 500 hPa, was shown. These results suggest that there may be two different block formation models, thus corroborating the concept proposed by L97. Our results were also similar to those of Illari (1984) in that they showed that the advection of low-QGPV (anticyclonic absolute vorticity) air into the block region at 300 hPa was crucial in maintaining their block. However, their diagnosis precluded any direct role that temperature advection played in block development or maintenance.

The relationship between blocks and precursor upstream cyclones, suggested by the conceptual model of Tsou and Smith (1990) which maintains that intervening jet streaks play a linking role between the cyclones and blocking anticyclones, was investigated in this study. The climatology of LS95a shows that block formation could be adequately explained by the Tsou and Smith (1990) block formation model for *all* cases examined. Tsou and Smith (1990) and LS95b found that these jet streaks involved with the formation of this blocking anticyclone strengthened significantly, perhaps in response to surface cyclogenesis, and that this jet streak was responsible for the anticyclonic vorticity advection field that caused ridge amplification. These features were also found in this study. This blocking episode, however, was associated with a subsequent upstream surface cyclone which appeared to intensify, or at least maintain, the block as had occurred during development. Thus, the location of the jet streaks within the large-scale flow relative to the block center appeared to be important. As long as jet maxima were located on the upstream flank, as in Tsou and Smith (1990), the block developed, intensified, or was at least maintained. However, when jet maxima were not configured in this manner (see sections 4 and 5), the block decayed.

The partitioned 500-hPa height tendency results showed that synoptic-scale processes, followed by planetary-scale processes, were largest in the block region that was examined. This was not in agreement with the results of LS95b or Tsou and Smith (1990), both of which showed that the interaction component was the largest, followed closely, or equaled by, the synoptic-scale component. Thus, it is possible that these differences reflect differences between warm- and cold-season blocking since each study used the same technique. Section 6, however, demonstrated that 500-hPa height-rise maxima found on the anticyclonic side of the associated jet maxima were primarily comprised of S and I height rises, which were the prominent contributors to block development and intensification. Thus, a comparison of these and LS95b results suggest that the contribution by the upstream cyclones to block development were different. In the LS95b block, the upstream surface cyclone contributed to the strengthening of the height rises that in turn were associated with block development and intensification through the I component (supported by P), as was the case for the development of this block. The upstream cyclones also contributed to block formation (L97) and intensification (L97 and here) directly through the S or S and I components acting in concert. Additionally, the P component forced height rises *throughout* the short lifetime of this event, and, as Table 2 demonstrates, intensification or decay, was determined by the sign of S or S plus I. The importance of the synoptic-scale in block formation and maintenance agrees with the results of Illari (1984) who used temporally partitioned QGPV analysis at 300 hPa in their diagnosis. During decay, the P component was a prominent contributor in forcing height falls in the LS95b case, while in this case, the S and I height falls overcame P-component height rises. Finally, these partitioned results, like Illari (1984), Tsou and Smith (1990), and LS95b, suggest that while P processes play a role in block formation and maintenance, S and I processes are important as well.

REFERENCES

Agayan, G. M., and I. I. Mokhov, 1989: Quasistationary autumn regimes of the Northern Hemisphere atmosphere in FGGE. *Atmos. Ocean Phys.,* **25,** 1150–1156.

Alberta, T. L., S. J. Colucci, and J. C. Davenport, 1991: Rapid 500-mb cyclogenesis and anticyclogenesis. *Mon. Wea. Rev.,* **119,** 1186–1204.

Baker, W. E., S. C. Bloom, J. S. Wollen, M. S. Nestler, E. Brin, T. W. Schlatter, and G. W. Branstator, 1987: Experiments with a three-dimensional statistical objective analysis scheme using FGGE data. *Mon. Wea. Rev.,* **115,** 272–296.

Colucci, S. J., 1985: Explosive cyclogenesis and large-scale circulation changes: Implications for atmospheric blocking. *J. Atmos. Sci.,* **42,** 2701–2717.

——, 1987: Comparative diagnosis of blocking versus non-blocking planetary circulation changes during synoptic scale cyclogenesis. *J. Atmos. Sci.,* **44,** 124–139.

Dole, R. M., 1986: The life cycles of persistent anomalies and blocking over the North Pacific. *Advances in Geophysics,* Vol. 29, Pergamon Press, **29,** 31–70.

Egger, J., M. Metz, and G. Muller, 1986: Forcing of planetary-scale blocking anti-cyclones by synoptic-scale cyclones. *Advances in Geophysics,* Vol. 29, Pergamon Press, **29,** 183–198.

Frederiksen, J. S., 1982: A unified three-dimensional instability theory of the onset of blocking and cyclogenesis. *J. Atmos. Sci.,* **39,** 969–982.

Grotjahn, R., 1996: Vorticity equation terms for extratropical cyclones. *Mon. Wea. Rev.,* **124,** 2843–2858.

Illari, L., 1984: A diagnostic study of the potential vorticity in a warm blocking anti-cyclone. *J. Atmos. Sci.,* **41,** 3518–3525.

Konrad, C. E., and S. J. Colucci, 1988: Synoptic climatology of 500-mb circulation changes during explosive cyclogenesis. *Mon. Wea. Rev.,* **116,** 1431–1443.

Krishnamurti, T. N., 1968: A diagnostic balance model for studies of weather systems of low and high latitudes, Rossby numbers less than one. *Mon. Wea. Rev.,* **96,** 197–207.

Lupo, A. R., 1997: A diagnosis of two blocking events that occurred simultaneously in the midlatitude Northern Hemisphere. *Mon. Wea. Rev.,* **125,** 1801–1823.

——, and P. J. Smith, 1995a: Climatological features of blocking anticyclones in the Northern Hemisphere. *Tellus,* **47A,** 439–456.

——, and ——, 1995b: Planetary and synoptic-scale interactions dur-

ing the life cycle of a mid-latitude blocking anticyclone over the North Atlantic. *Tellus Special Issue: The Life Cycles of Extratropical Cyclones,* **47A,** 575–596.

——, ——, and P. Zwack, 1992: A diagnosis of the explosive development of two extratropical cyclones. *Mon. Wea. Rev.,* **120,** 1490–1523.

Mullen, S. L., 1987: Transient eddy forcing and blocking flows. *J. Atmos. Sci.,* **44,** 3–22.

Quiroz, R. S., 1984: The climate of the 1983–1984 winter—A season of strong blocking and severe cold over North America. *Mon. Wea. Rev.,* **112,** 1894–1912.

Rausch, R. L. M., and P. J. Smith, 1996: A diagnosis of a model-simulated explosively developing extratropical cyclone. *Mon. Wea. Rev.,* **124,** 120–130.

Rex, D. F., 1950a: Blocking action in the middle tropospheric westerlies and its effect upon regional climate I: An aerological study of blocking action. *Tellus,* **3,** 196–211.

——, 1950b: Blocking action in the middle tropospheric westerlies and its effect upon regional climate II: The climatology of blocking action. *Tellus,* **3,** 275–301.

Rogers, E., and L. F. Bosart, 1991: A diagnostic study of two intense oceanic cyclones. *Mon. Wea. Rev.,* **119,** 965–996.

Rolfson, D. M., and P. J. Smith, 1996: A composite diagnosis of synoptic-scale extratropical cyclone development over the United States. *Mon. Wea. Rev.,* **124,** 1084–1099.

Schubert, S. D., R. D. Rood, and J. Pfaendtner, 1993: An assimilated dataset for earth science applications. *Bull. Amer. Meteor. Soc.,* **74,** 2331–2342.

Shapiro, R., 1970: Smoothing, filtering, and boundary effects. *Rev. Geophys.,* **8,** 359–387.

Shutts, G. J., 1983: The propagation of eddies in diffluent jetstreams: Eddy vorticity forcings of blocking flow fields. *Quart. J. Roy. Meteor. Soc.,* **109,** 737–761.

——, 1986: A case study of eddy forcing during an Atlantic blocking episode. *Advances in Geophysics,* Vol. 29, Pergamon Press, **29,** 135–161.

Tibaldi, S., and F. Molteni, 1990: On the operational predictablity of blocking. *Tellus,* **42A,** 343–365.

——, P. Ruti, E. Tosi, and M. Maruca, 1993: Operational predictability of winter blocking: An ECMWF update. *Proc. ECMWF Seminars on Validation of Forecasts and Large-Scale Simulations over Europe,* Reading, Berkshire, United Kingdom, ECMWF.

——, E. Tosi, A. Navarra, and L. Pedulli, 1994: Northern and Southern Hemisphere seasonal variability of blocking frequency and predictability. *Mon. Wea. Rev.,* **122,** 1971–2003.

Tracton, M. S., 1990: Predictability and its relationship to scale interaction processes in blocking. *Mon. Wea. Rev.,* **118,** 1666–1695.

Tsou, C.-H., and P. J. Smith, 1990: The role of synoptic/planetary-scale interactions during the development of a blocking anticyclone. *Tellus,* **42A,** 174–193.

Zwack, P., and B. Okossi, 1986: A new method for solving the quasigeostrophic omega equation by incorporating surface pressure tendency data. *Mon. Wea. Rev.,* **114,** 655–666.